



Short review

Metal-assisted chemical etching for designable monocrystalline silicon nanostructure



Meicheng Li^{a,c,*}, Yingfeng Li^a, Wenjian Liu^a, Luo Yue^b, Ruike Li^a, Younan Luo^a, Mwenya Trevor^a, Bing Jiang^a, Fan Bai^a, Pengfei Fu^a, Yan Zhao^c, Chao Shen^c, Joseph Michel Mbengue^a

^aState Key Laboratory of Alternate Electrical Power System with Renewable Energy Sources, North China Electric Power University, Beijing 102206, China

^bChina University of Petroleum, Beijing 102249, China

^cChongqing Materials Research Institute, Chongqing 400707, China

ARTICLE INFO

Article history:

Received 30 December 2015

Accepted 3 January 2016

Available online 7 January 2016

Keywords:

A. Nanostructures

A. Semiconductors

B. Chemical synthesis

ABSTRACT

Metal-assisted chemical etching (MACE) is a simple, low-cost and versatile method of fabricating various silicon nanostructures. Due to the etching anisotropy of monocrystalline silicon, i.e. its different crystal orientation has different number of silicon back bonds needed to be broken in the etching process, the obtained silicon nanostructures are morphology variable. It has been demonstrated that, by choosing the species or morphologies of catalyst, adjusting the etchant composition or concentration, changing the doping species and level of the silicon substrate, or introducing extra physical fields, MACE method can be used to prepare various desired silicon nanostructures. This review summarizes the most recent contributions in the fabrication of designable monocrystalline silicon nanostructure by MACE. In order to provide a relatively complete comprehension of the MACE, the fundamental principle and basic manipulation process of a conventional MACE, as well as the main influence factors on the etching effects are given; and the common applications of MACE in silicon etching are briefly reviewed. This article also presents some new developed improved MACE technologies and their potential applications in the extended field.

© 2016 Elsevier Ltd. All rights reserved.

1. Introduction

The approaches for the fabrication of silicon nanostructures can be briefly classified into two schemes, the bottom-up and top-down ones. For the bottom-up scheme, the most representative method is the ‘vapour–liquid–solid’ (VLS) growth [1–6]. In this method, catalytic liquid alloy phase is introduced as the seed, which can catalyze the dissociation of the silicon gas with the freed silicon atoms, rapidly adsorbing them to supersaturating levels; then, the silicon atoms dissolve out and arrange to crystalline silicon nanostructures. As the VLS growth is a quasi-stationary thermodynamics process, it can be used to fabricate relatively high-quality silicon nanowires (SiNWs). The top-down scheme can be further separated into dry and wet etching approaches. The most commonly used dry etching approach is the inductively coupled plasma (ICP) etching [7,8], which utilizes plasma reaction

gas to etch the silicon substrate with mask and can provide fairly good etch rates and anisotropy. And the typical wet etching approach is the metal-assisted chemical etching (MACE) method [9–17], in which the silicon substrate immersed in the etchant is etched into various nanostructures with the assistance of metal catalyst.

Cost-efficiency and equipment requirement are two factors must be considered, for the widespread applications of every approaches mentioned above. The VLS and ICP methods both require large equipment, so they cannot be afforded by most laboratories. Additionally, the processes of them are high-cost, since they both need high purity gases, vacuum technology and high temperature (or high power magnetic coil); moreover, they also have a certain dangerous nature because they both require inflammable dangerous gases. Due to these negative factors, only a few of research teams still use the VLS and ICP methods in fabrication silicon nanostructures. Conversely, the MACE method is thriving and developing day by day, since it only requires very simple equipment (a beaker), and the silicon nanostructures prepared by this method are designable by adjusting the etching process.

* Corresponding author at: North China Electric Power University, State Key Laboratory of Alternate Electrical Power System with Renewable Energy Sources, Beijing 102206, China. Fax: +86 1061772951.

E-mail address: mcli@ncepu.edu.cn (M. Li).

MACE is a reaction process in aqueous solution, so the silicon substrate is in full contact with the etchant, and meanwhile, the catalyst (metal particle) is mobile following the micro flow of the solution [18]. These make the motive path of the catalyst, which determines the morphology of etched silicon nanostructures, is difficult to be controlled. Recently, a lot of effort has been made on studying the etching mechanism, as well as the main factors influencing the etching effects in MACE [19–26]; and based on these in-depth understandings, a lot of processes to realize the designability and controllability for the etched silicon nanostructures have been developed. Briefly, these processes can be classified to five categories: adjusting the species and morphology of the catalyst, changing the recipe of the etchant, modifying the doping element and level of the silicon substrate, introducing extra physical fields, and executing post-process for the obtained nanostructures. Besides, one research group has even improved the MACE technology to vapor phase condition [18]. Today, MACE technique has advanced to a level where desired architectures and surface quality can be readily fabricated, hence is becoming one of the main technologies in preparing silicon nanostructures.

In this review, we first discuss the basic manipulation process and fundamental principle of MACE, as well as the main factors influencing the etching effects. Then, the common application in silicon etching is briefly introduced. Next, efforts are made to summarize the most recent contributions in the fabrication of designable monocrystalline silicon nanostructures by MACE. Finally, some new improved MACE technologies and their applications are simply introduced.

2. Manipulation process and fundamental principle of MACE

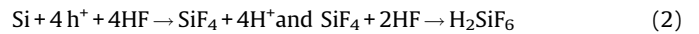
MACE is a very simple technique in fabricating silicon nanostructures. The basic manipulation of it even only requires a beaker. The manipulation process can be briefly separated into three steps [27]: Firstly, cleaning the silicon substrate and configuring the etching solution for later use; then, immersing the silicon substrate into the etching solution and maintaining a period of time; finally, taking the silicon substrate out and rinsing it with deionized water. Such a simple technique can be afforded in any laboratory, and meanwhile can be used to prepare many interesting silicon nanostructures with low cost.

The underlying physical mechanism in MACE process is also very simple, which can be briefly reflected by the following equations [27]:

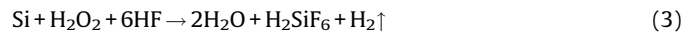
Reaction at metal (cathode)



Reaction of Si etching (anode)



Overall equation



The reaction details, however, are a bit more complex, as given in Fig. 1. When the silicon substrate is immersed into HF/AgNO₃ solution, the Ag⁺ ions near the silicon surface will seize electrons from the valence band of silicon, leading to the formation of Ag nucleation. As the reaction progresses, Ag nucleation gradually grows into Ag nanoparticles. Thereafter, Ag nanoparticles directly seize electrons from their contact or around silicon locations because the electronegativity of Ag is higher than silicon, creating a hole-rich region beneath and around the catalyst. Then, H₂O₂ is reduced at Ag nanoparticles; and the holes are consumed by the oxidation of silicon to silica, which is quickly dissolved by the HF. The Ag nanoparticle travels into the silicon wafer as the silica layer is dissolved, thus the depth of the Ag nanoparticles in the pit increase gradually with the increase of reaction time.

Although the fundamental physical and chemical process of MACE is very simple, there are also many factors in the etching process that are adjustable. Since the main objects involved in the MACE process including the silicon substrate, the catalysts and etchant, the efforts for modifying the etching process are all carried out on these three aspects. The main parameters for silicon substrate that can be adjusted are the doping element and doping level, which dramatically affects the etching rate and porosity of silicon nanostructures. Canevali et al. [23] have demonstrated that the silicon nanowires formation rates increase with dopant concentration; meanwhile Geyer et al. [22] found that the porosity of the etched nanowires can be controlled by the doping level of the silicon wafer. In addition, the surface wettability of the silicon substrate also has great influence on the etching results [28]. For instance, Bai et al. [29] proposed that the UV/ozone pretreatment of the silicon substrate can form a very thin SiO₂ layer, which can improve the uniform nucleation of Ag nanoparticles on the Si surface, thus induce the formation of the silicon nanowire arrays with good uniformity and high filling ratio. For catalysts, Ag and Au are used most commonly. They bring in obvious different etching process and features. As silver is soluble in H₂O₂ and HF solution, before the actual etching process, it is first dissolved and then recrystallize to form small nanoparticles [27,30]. This physical character on one hand enhances the etching rate since small nanoparticles are in better contact with the silicon substrate; on the other hand it also results in poor controllability of the etching process. Additionally, since the hole-generating rate of Ag just matches the etching (reaction) rate, the surface of the obtained silicon nanostructure is nearly smooth. Au has better chemical inertia, so its original morphology is unchanged in the etching

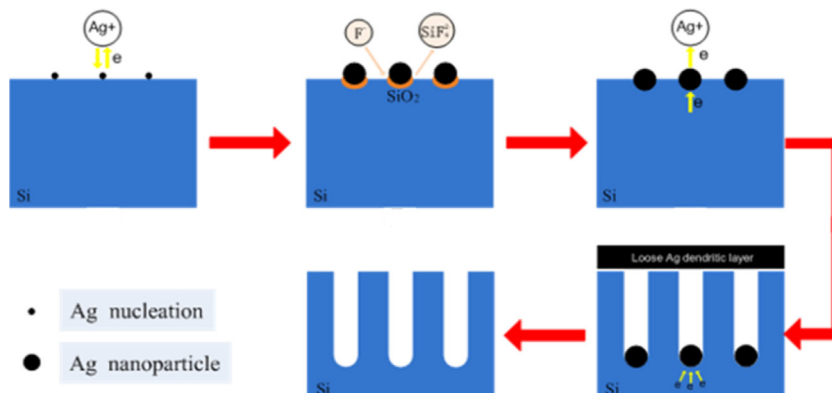


Fig. 1. Schematic illustration of the etching mechanism of silicon nanostructures by MACE in HF/AgNO₃/H₂O₂ solution.

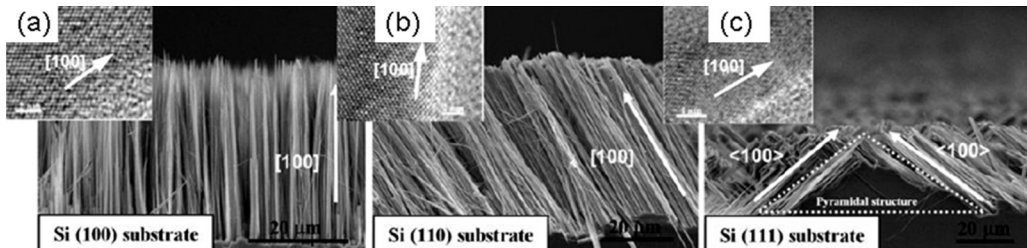


Fig. 2. SEM images of SiNW arrays fabricated on silicon substrates of different orientations. (a) Si (100), (b) Si (110) and (c) Si (111) substrate. The insets are high-resolution TEM images, which indicate that the SiNWs are single-crystalline [51,52].

process. Therefore, it is difficult to obtain high etching rate using Au as the catalyst, but it provides the possibility to control the architecture of the silicon nanostructure by designing the morphology of the catalyst. Different from Ag, the hole-generating rate of Au is much higher than the consumption rate in the etching reaction. The redundant holes diffuse to the areas on the silicon substrate far from the catalyst and result in porous structures. Besides, the shape and size of catalyst can also have great influence on the etching direction thus the morphology and shape of the obtained nanostructures [21]. For the etchant, the etchant composition is the most important parameter. According to above reaction equations, it can be easily deduced that increasing the H₂O₂ can increase the hole injection current thus lead to high rate etching. Chartier et al. [31] found that the increased H₂O₂ concentration could also increase the distance holes can travel within the silicon, leading to straight, tight holes, to conical holes, crates. A study by Bai et al. [27] suggests that the porosity of the silicon nanowires become more obvious when the concentration of H₂O₂ became higher. Recently, Hildreth et al. [21] claimed that the etching path (direction) also shows great dependence on the ratio between the HF and H₂O₂. Except for the etchant composition, the wettability between the etching solution and the silicon also has influence on the etching results. From the reaction equations it was found that H₂ is generated in the etching process. Such generated H₂ produces bubbles that adhere to the surface of silicon. During the release of these bubbles, some of them will burst thus bring in stripes on the surface of the silicon nanostructures. Hen et al. [11,32] found that adding moderate ethanol in the etchant can effectively improve the contact between the etchant and the silicon substrate thus avoid the generation of H₂ bubbles.

Despite the mechanisms in note MACE being relatively thorough and the main influence factors on the etching results are basically clear, there are still some fundamental problems that have not been resolved. For instance, consensus on the mass transfer process of the silicon atoms during the etching has not been reached. Peng et al. [10,33] assumed that the reagent and reaction product diffuse along the interface between the noble metal and the wall of the etching structure; while Werner et al. [34] supported that in the etching process the silicon atoms

dissolve into the metal and diffuse through the metal and are then oxidized on the surface of the metal. These two inferences both have seemingly “solid” basis, so it is difficult to give a definite conclusion. On this issue, our experimental results tend to support the latter conclusion. An accurate understanding on this process will provide significant guidance for the design and fabrication of novel silicon nanostructures.

3. Common applications of MACE in silicon etching

From being developed, the most common applications of MACE are to fabricate various vertical, large aspect ratio SiNWs and silicon Si nanoholes (SiNHs). Of them, SiNW has been widely used for light-trapping in photovoltaic devices [35–38] and been regarded as one of the most attractive building blocks for many future optical and optoelectronic devices [39–47]; SiNH can be also effectively used to enhance light harvesting in solar cells [48], like the famous black silicon solar cells [49,50]. There are abundant reports that have been published on this issue. Here, we just briefly reviewed some representative literature and some works of our group, so that the reader can have an intuitive understanding on the application of MACE but we did not pursue summarizing all of the articles related.

3.1. SiNW obtained by MACE

MACE is a local electrode less chemical reaction process; therefore, the etching morphology of silicon by MACE is determined by the shape and motivation path of the catalyst. If the catalyst is a continuous thin film with nanoscale porous on the silicon substrate, SiNW should be obtained. In MACE of crystalline silicon, the reaction rate shows great anisotropy (crystal orientation selectivity), since the numbers of Si—Si bonds needed to be broken along different directions are quite different. For instance, as illustrated in Fig. 2a–c, <100> direction is the preferential etching direction of Si in MACE [51,52].

However, by adjusting some factors like the molarity ratio of HF to H₂O₂ [25,53], the etching direction can be effectively controlled. Via nanosphere lithography, Peng et al. [54] have fabricated ordered SiNW on p-type Si wafers. They first deposited a

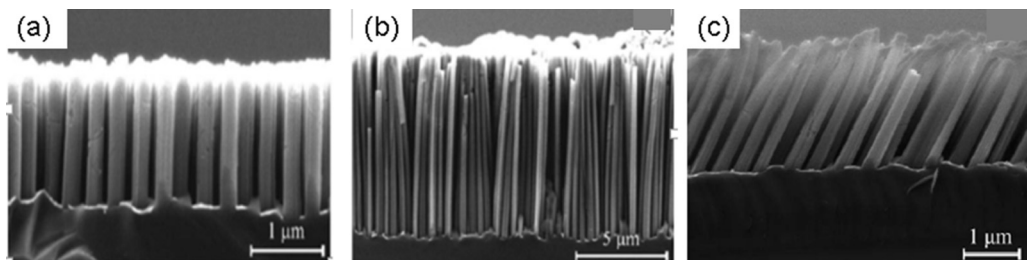


Fig. 3. SEM images of SiNW arrays fabricated on (a) Si (100), (b) Si (111) and (c) Si (113) wafers [54].

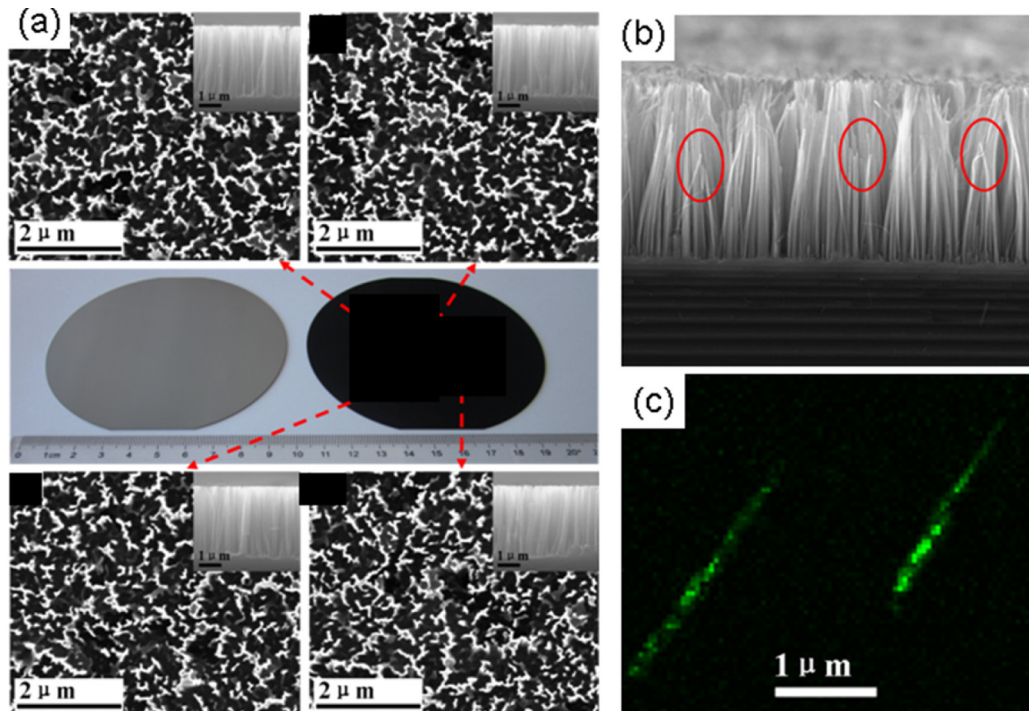


Fig. 4. (a) Wafer-scale SiNW arrays on n-type Si (100) by template-free MACE; (b) porous p-type SiNW arrays and (c) the photoluminescence images of it (individual nanowire) [29].

monolayer of silica colloidal crystal on the surface; then by chemical etching in 50:1HF solution, the 2D non-close-packed silica colloidal crystal was fabricated; thirdly, a metal layer was deposited onto silicon surface; after that, the silica templates were removed by brief ultrasonication in water; finally the silver film with periodic nanoholes was used as catalyst for etching. The obtained SiNW arrayson Si (100), Si (111) and Si (113) wafers are shown in Fig. 3a–c, respectively.

Without using a template, Bai et al. [29] fabricated wafer-scale SiNWs on Si (100) wafer. As shown in Fig. 4, the SiNW array is of high filling ratio ($1.1 \times 10^{10} \text{ cm}^{-2}$) and good uniformity. Through charactering the reflection spectra on 30 dots on the surface, the uniformity of the SiNW arrays is estimated to be below 0.2 of the relative standard deviation. They have also fabricated SiNW arrays on lightly dopedp-type Si (100) wafers (resistivity of 7–13 Ω cm), and obtained porous samples with circular nanopores (diameter about 5 nm) on the sidewall [27]. Such porous SiNW can emit strong green fluorescence.

3.2. SiNH fabricated by MACE

If the catalysts are discrete nanoparticles distributing on the silicon surface, the obtained silicon nanostructures should be various SiNHs [55–57]. One usually used method to prepare the catalysts is the silver mirror reaction method, where the silver nanoparticles are electrolessly deposited on the silicon surface in a mixed solution of AgNO_3 and HF [49], or of $[\text{Ag}(\text{NH}_3)_2]\text{OH}$ and glucose [58] at room temperature. After silver mirror reaction, the obtained silver nanoparticles are always of various shapes (Fig. 5a) [59]. However, the shape of the NH should be influenced but not determined by the shape of the catalysts. If the ratio of $\text{H}_2\text{O}_2:\text{HF}$ is low (2.9:1), the shape of the nanoholes is square on Si (100) (Fig. 5b) or hexagon on Si (111) (Fig. 5c) surface [16]. These show clearly that the shape of the NH is determined by the anisotropy of silicon. Another proof for this conclusion is that, on a (110) substrate the etch patch moves along an allowed $<110>$ direction

(i.e., $[\bar{1}00]$ or $[0\bar{1}0]$) at random (Fig. 5d) [60]. However, when the ratio of $\text{H}_2\text{O}_2:\text{HF}$ is high (5:1), the etching rate became very fast thus the shape of the obtained SiNHs are all quasi-round shape (Fig. 5e).

For the fabrication of SiNH, since the catalysts are isolated nanoparticles, their motivation path depends more on the anisotropic etching for different crystal orientation of silicon, the dislocation defects in the substrate, as well as the micro flow of the etchant and the H_2 bubbles generated. As a consequence, despite following the same mechanism as SiNW etching, the SiNH morphologies become more complex. For example, various helical nanopores (Fig. 6) as prepared by Jiang et al. [61] could be obtained when the HF concentration is greater than 40%. We attribute the formation of helical pores to the rotation or revolution of Ag particles, which related to the dislocation defects, etching rate (HF concentration), gravity and other factors. Detailed studies on the influence factors on the etching morphologies are of great help for the designable fabrication of the Si nanostructures.

4. Designable monocrystalline silicon nanostructure fabricated by MACE

For the more practical and specific application of silicon nanostructures, it is required to control the size, morphology and surface quality of the nanostructures. To achieve the rational design and fabrication of various silicon nanostructures, we can take advantage of the anisotropy etching of silicon accompanied by adjusting the substrate quality, catalyst and etchant, as well as by post processing [62]. Next, we summarize the most recent contributions in the fabrication of designable monocrystalline silicon nanostructures by MACE.

4.1. SiNWs array with certain diameter and pitch

For SiNWs array, the designable size parameters mainly mean the diameter, pitch and length. The length of SiNW, being related to

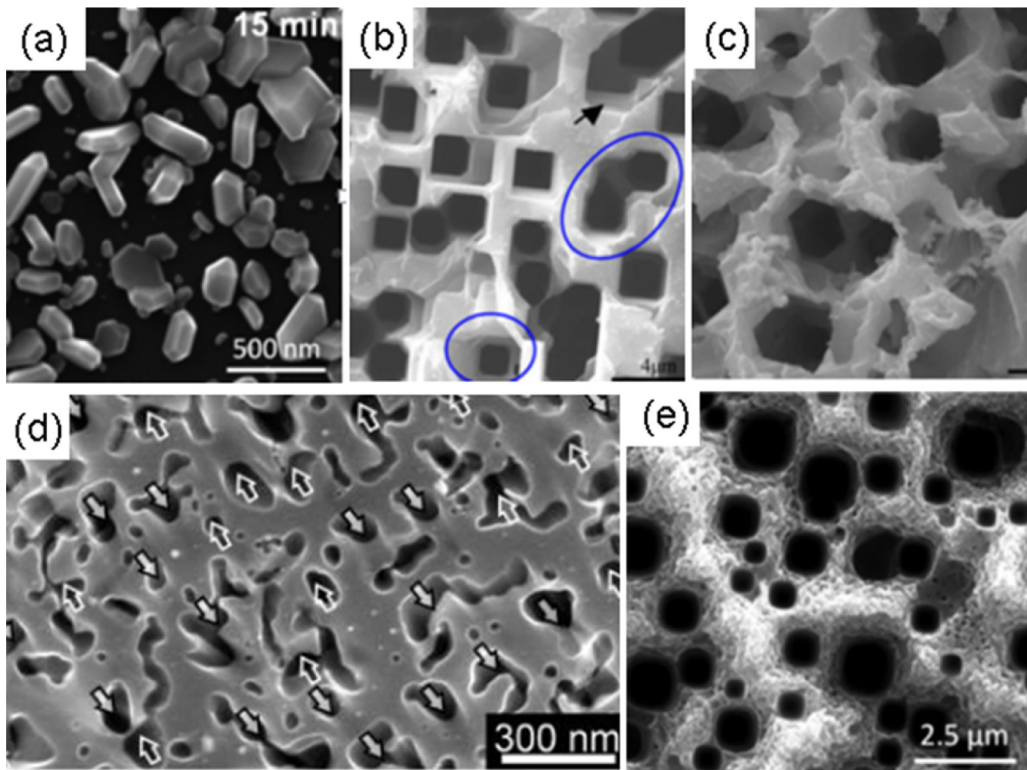


Fig. 5. (a) Silver nanoparticles of various shapes fabricated by silver mirror reaction [59]; (b) square NHs on Si (100), (c) hexagonal on Si (111) surface [16], and (d) etch patches of random allowed <110> directions on Si (110) substrate etched by etchant owning low H₂O₂:HF ratio [60]; (e) quasi-round NHs obtained in etchant of high H₂O₂:HF ratio.

the etchant concentration and etching temperature, is proportional to the etching time thus can be simply controlled [63]. The etching morphology dramatically depends on the motivation trajectories of the metal catalyst; therefore, a most direct approach to control the morphology of the obtained structure is to control the morphology of the catalyst. This is just the basic starting point of the template method. Until now, several methods have been developed to fabricate the template (mask) of the etching, including the photoresist mask, anodic aluminum oxide mask, PS sphere mask, SiO₂ sphere mask, PMMA mask and CsCl mask Huang et al. [15,64–70]. Of them, the PS sphere mask is most widely used in laboratory.

The overall fabrication process using the PS sphere mask method is schematically depicted in Fig. 7a [71]. In this process, the key step is to assemble the PS sphere arrays on the silicon surface. Very recent, Gao et al. [73] have reported a novel method to fabricate large area ($1\text{ m} \times 1\text{ m}$) uniform PS mask. After the PS sphere array is prepared, a step to RIE the PS spheres is carried out to form the spacing, and then an Ag thin film is deposited and the PS spheres are removed, after that the MACE of silicon starts. Using this method, very regular SiNW arrays can be obtained as shown in Fig. 7b and c [66,72]. It can be noted that, the metal film still maintains its integrity as shown in Fig. 7b and c. Similarly, Liu et al. [74] have found that the

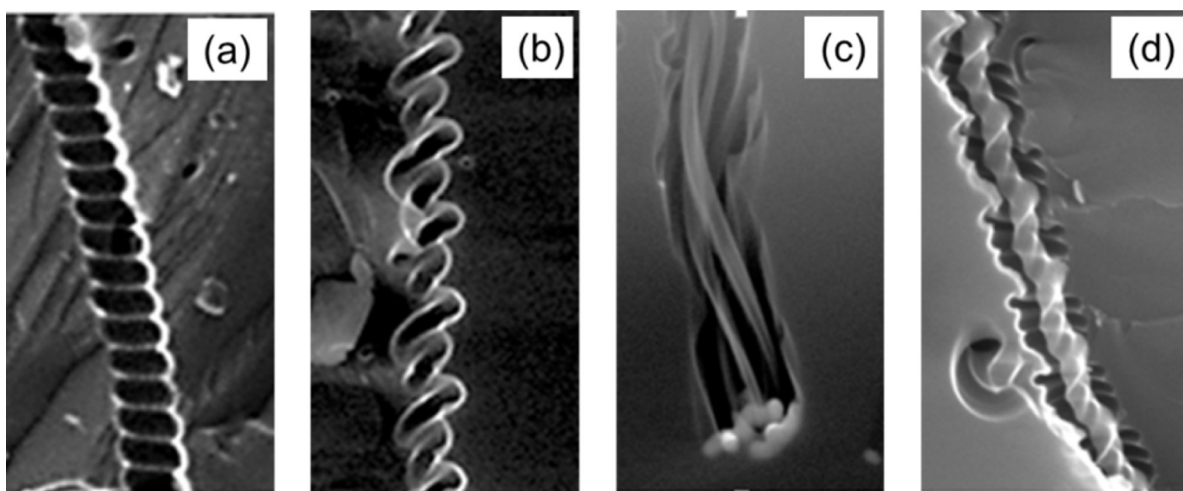


Fig. 6. Cross-sectional SEM micrographs of various helical NHs of different morphologies, etched by etchant with HF concentration greater than 40% [61].

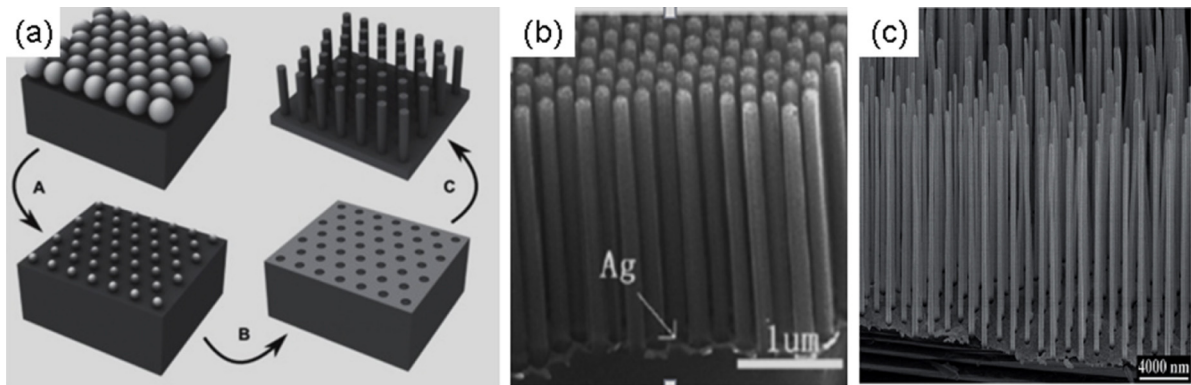


Fig. 7. (a) An overall MACE process using PS spheres as the mask [71]; and the regular SiNW arrays of (b) high and (c) low surface concentration obtained by this method [66,72].

morphologies of the etched SiNW and SiNH arrays matched well with those of the Ag holes and nanoparticles. These demonstrate the importance of the catalyst in fabricating silicon nanostructures with desired parameters.

Using template method can get accurate silicon nanostructures, while the fabricating of mask is always time-consuming, expensive and to some extent not easy to be mastered. Therefore, using the template free method to realize the control of the SiNW parameters attracts many interesting. Through thermal annealing of thin Ag film, Liu et al. [74] have successfully prepared semispherical Ag nanoparticles and Ag mesh with holes (Fig. 8a and b). After MACE, sparse individual SiNHs and SiNWs can be obtained as given in Fig. 8c and d. They demonstrated that the diameter and distribution of mesh holes as well as the nanoparticles are manipulatable by the film thickness or the annealing temperature. Therefore, the diameter and pitch can be also tuned

by controlling the respective catalyst. However, until now there is still no report on controlling the diameter and pitch separately, as well as controlling the periodicity of SiNW nanostructures by template free method. This is still a great challenge for the researchers in this field.

4.2. Si nanostructures with various diameters from top to bottom

Recently, several simulation results denote that tapered SiNW shows much enhanced light harvesting capability than cylindrical one [75,76], due to its continuous diameter thus resonant wavelengths excited. Using well-designed mask combined with RIE method, Lu and Lal [77] have fabricated high-efficiency silicon nanoconical frustum array solar cells. Therefore, fabrication of tapered SiNW by the simple MACE method attracts a lot of attention.

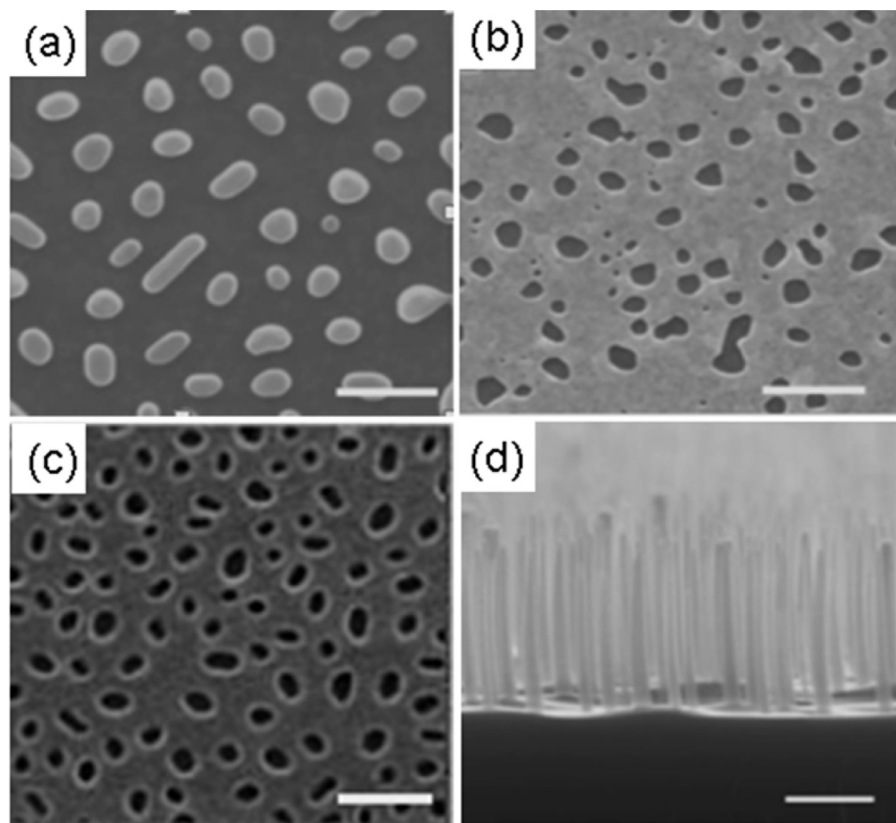


Fig. 8. SEM images of (a) separated silver nanoparticles, (b) silver mesh with holes and the corresponding (c) SiNHs and (d) SiNWs after etching [74].

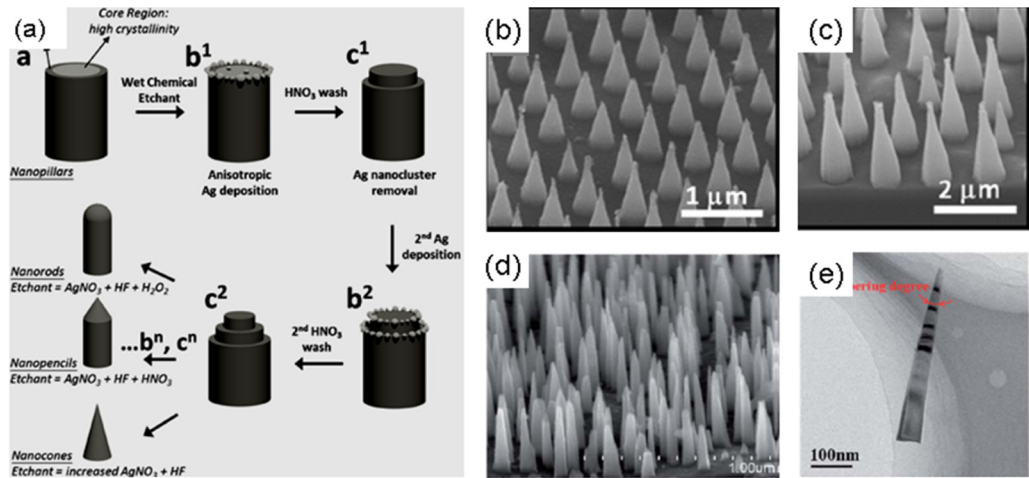


Fig. 9. (a) Schematic illustrations of the operation process to fabricate Si nanostructures with different morphologies, and SEM images of the tapered silicon nanostructures (b and c) obtained by this process [78]; (d) SEM images of tapered SiNW arrays fabricated by a one-step template-free method and (e) TEM images of one individual tapered SiNW [78].

Lin et al. [78] have developed a relative complex method to fabricate silicon nanocone. The schematic is illustrated in Fig. 9a. Firstly, silicon nanopillars are prepared by HF/H₂O₂ solution using a Ti/Au mesh film as the mask. Secondly, the nanopillars are etched by [AgNO₃ + HF + HNO₃/H₂O₂]. In this etching process, first, the Ag catalysts are deposited on the tip of the obtained pillars with obvious site selectivity through a silver mirror reaction; then, the etching process takes place. When the second etching process is carried out repeatedly, the silicon nanocone arrays are obtained, as given in Fig. 9b and c.

Bai et al. [79] have developed a one-step template-free method to realize the fabrication of tapered SiNW arrays with various filling ratios. In their work, they first deposited a silver film on the silicon surface and then carried out etching using HF/H₂O₂ solution as the etchant. The key mechanism for obtained tapered SiNW is the in-situ oxidative dissolution of the silver network in the etching process. Since the standard reduction potential of oxidizing agents in the solution is greater than that of silver, the silver network is gradually dissolved (oxidized to silver ions) and shrunk during its sinking process. Besides, the diffusion of positive holes from the bottom to the sidewalls can also contribute to the formation of the tapered SiNW and SiNH arrays [31,61,80]. The obtained tapered SiNWs with tapering degree about 12.7° are given in Fig. 9d and e.

Except above methods, there are also some post process methods to fabricate tapered SiNWs. For instance, Jung et al. [81–83] found that the tapering can be done by KOH etching for about 60 s after the SiNW has been prepared, as shown in Fig. 10. In

addition, during this step, the bunched SiNW arrays, induced by van der Waals forces, can be easily separated from each other.

4.3. Zigzag SiNW

It has been demonstrated that the etching direction of Si can be effectively controlled by adjusting some factors like the molarity ratio of HF to H₂O₂ [13,25]. By imposing vertical gradient of etchant (HF and H₂O₂) concentrations during the etching process, Kim et al. [84] first fabricated structurally well-defined zigzag SiNWs on (100)-oriented silicon wafers, as shown in Fig. 11. The vertical gradient of etchant is introduced by a thin layer of porous silicon nanostructures covering the entire mesh surface, which is fabricated by a first-step etching. This step etching is carried out after the Au mesh being prepared, in etchant of high relative H₂O₂ concentration. The high H₂O₂ concentration results in an extra amount of positive holes, which can readily diffuse away from the etching front to the lattice defects and dopant sites, thus resulting in the formation of the thin layer of porous silicon nanostructures.

How does this thin layer can impose vertical gradients of etchant concentrations? Kim et al. [84] gives a rational explanation from the view of microscopic electrochemical events. Chemical etching will quickly deplete H₂O₂ near the etching front thus establishes a large concentration gradient of H₂O₂ along the direction perpendicular to the action interface. Depletion of H₂O₂ at the etching front in turn results in retardation of etching reaction. At this stage, a new cycle begins by the influx of H₂O₂ due to the vertical diffusion of the etchant. Iteration of the cycle

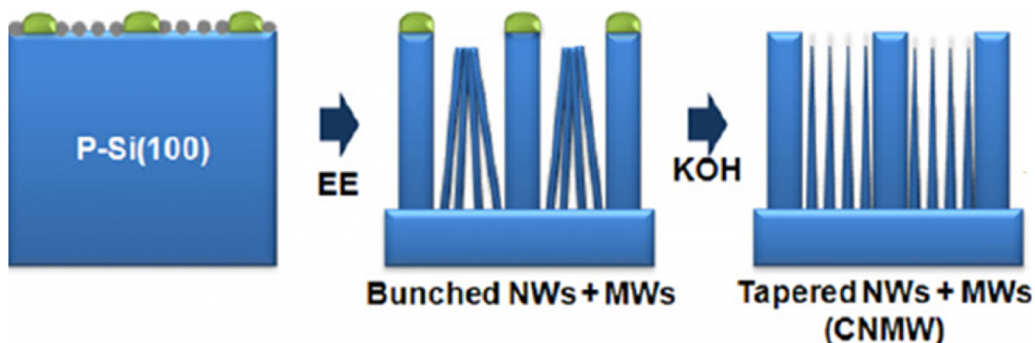


Fig. 10. Schematic illustrations of the operation process to fabricated tapered SiNWs by a post process method of immersing in KOH solution for about 60 s [81–83].

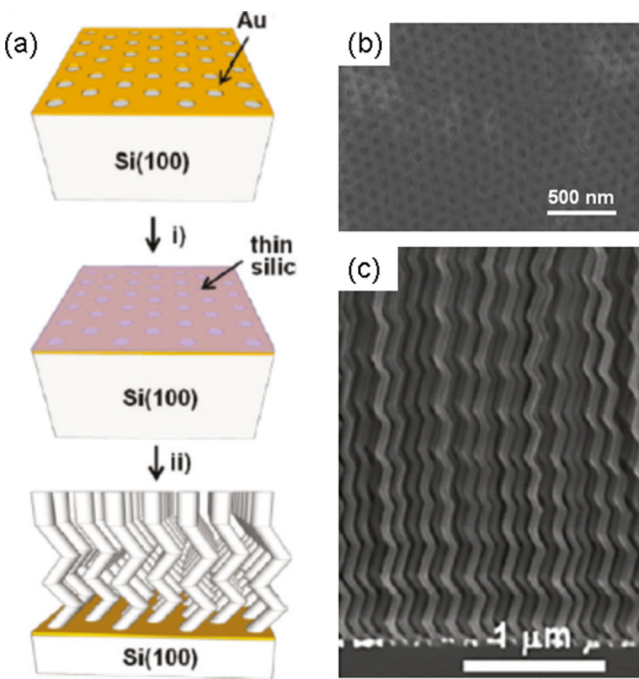


Fig. 11. (a) An overall flow of fabrication zigzag SiNW arrays; (b) SEM images of the thin layer of porous silicon nanostructures after the first step etching; (c) SEM images of the zigzag SiNW arrays obtained [84].

corresponds to the periodic oscillations of etchant concentration, which switches the etching directions, that is, etchings along the vertical $<100>$ direction at low H_2O_2 concentration and non- $<100>$ directions at high concentration.

The relationships between the H_2O_2 concentration and the etching directions can be explained as follows. The second-step etching is carried out in etchant of low relative H_2O_2 concentration at high temperature. In this case, if the H_2O_2 concentration at the reaction front is high, due to the high temperature, the decomposition of H_2O_2 is fast thus abundant holes can be generated. Therefore, silicon atoms of more compact crystal

planes with higher density of silicon back bonds than (100) surface become labile to the oxidation, resulting in etching along non- $<100>$ directions. In contrast, if the H_2O_2 concentration is low, no sufficient holes can be generated thus only the least compact (100) surface with the fewest silicon back bonds can be etched. The uniform etching direction by the different locations of the Au film in every oscillation is related to the integrity of the Au film during the etching process. However, if we change the Au film into nanoparticles, the obtained nanohole arrays are expected to be of the same directions yet, due to the interactions between adjacent catalysts [85,86].

4.4. Multilayer and periodic porosity-patterned SiNW

For the transfer of uniform, vertically aligned SiNW to foreign substrates, an important problem is that the SiNWs will fracture at random locations. Weisse et al. [87] found that by introducing an intermediate process in the MACE of silicon, they could fabricate a designated segment of vertically aligned SiNW arrays.

The fabrication procedure for the cracked SiNW array is given in Fig. 12. Once the SiNW of desired length was achieved by controlling the etching time, the silicon wafer was rinsed in deionized water and dried. Subsequently, the silicon wafer was soaked in a 75 °C DI water bath for about three hours to delaminate the Ag film. After that, the wafer was returned into the etching solution. At the start of the second step etching a well-controlled horizontal crack parallel to the wafer surface was formed; then the etching continued to elongate the SiNWs. This intermediate process can be carried out more than one time, and SiNWs with several horizontal cracks can be obtained, as in Fig. 12b and d.

4.5. Ultrathin SiNW

Functional ultrathin SiNWs are of promising applications in high-tech devices, such as high responsive photo-detectors and ultra-high sensitive bio-chemical sensors. Very recent, Li et al. [88] reported that using an Au/Ag bilayered metal mesh as the catalyst can obtain ultrathin SiNWs of porous structures. They explained the etching as a double-screen process, as shown in Fig. 13. As the Au and Ag nanofilms are deposited with no template in sequence,

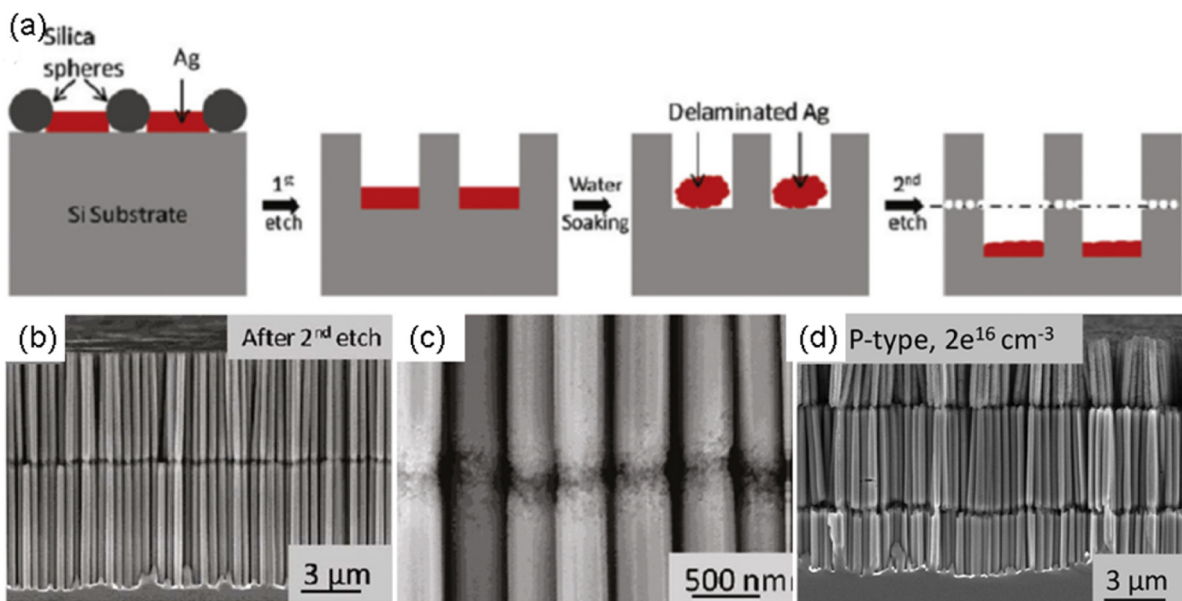


Fig. 12. (a) The fabrication procedure of the cracked SiNW array; (b) SEM images of the etched SiNW arrays with one horizontal crack and (c) the zoom-in view of the crack; (d) SiNW arrays of two horizontal cracks [87].

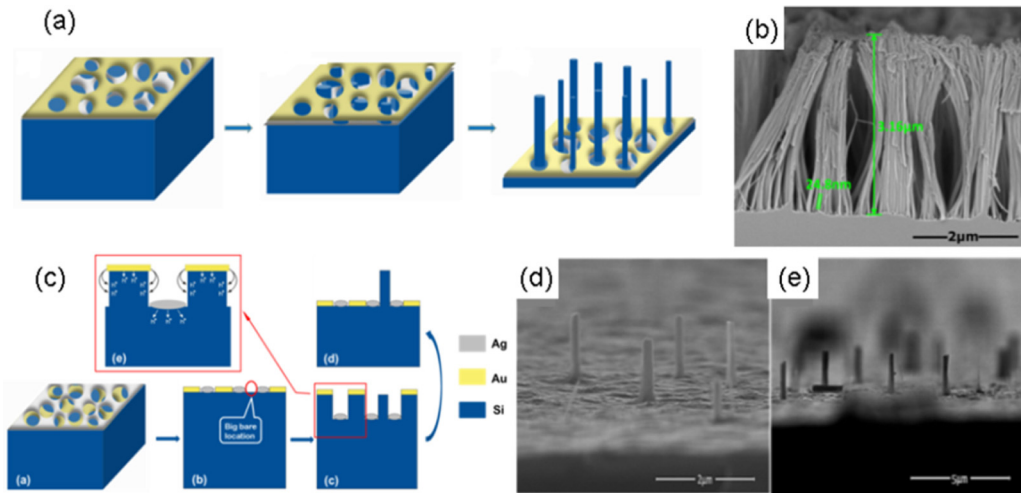


Fig. 13. (a) The schematic diagram of the Ag(nether)/Au(upper) nanofilm catalytic etching process, and (b) SEM image of the porous ultrathin SiNW array obtained; (c) illustration of the etching process using the Au(nether)/Ag(upper) bilayer nanofilm and (d and e) the obtained sparse silicon pillars [88].

their meshes overlapped. During the following etching process, firstly, the Ag mesh etches the silicon into vertical SiNWs; soon afterwards, the Au re-etches the SiNWs into ultrathin porous ones. The SEM image of their obtained porous ultrathin SiNW array is shown in Fig. 13b.

However, when they deposited the Ag film on the Au one, the etching process is quite different. As mentioned above, the silver catalyst may undergo a first solution then recrystallize process in this case; the etching process is illustrated in Fig. 13c. The silver nanofilm first transforms into nanoparticles, which then penetrate into the interspaces of the Au nanofilm and etch the silicon substrate into SiNWs; after that, the SiNWs are etched and vanished by the Au nanofilm but only some sparse silicon pillars are left, which correspond to the very large holes on the Au mesh. The obtained results are given in Fig. 13d and e.

Another method to fabricate ultrathin SiNWs is carried out in a two-step dry oxidation and post-chemical etching process for the obtained vertical thick SiNW. The dry oxidation is executed at temperatures 750–850 °C in a tube furnace to generated core–shell SiNW arrays. Then, the oxide layer of the core–shell SiNW array is removed by the HF solution. Using this approach, Su et al. [66] have successfully fabricated core–shell SiNW arrays with gradually reduced diameters (Fig. 14). The inner diameter can be reduced down to sub-10 nm by controlling the oxidation time (Fig. 14c).

4.6. Co-integrated wire structure of MWs and NWs(CNMW)

Co-integrated wire structure of MWs and NWs shows specific application promising in fabricating solar cells architected by both

radial and bulk p–n junctions [83], as shown in Fig. 15a. Where the red color denotes the n-type shell and the blue color denotes the p-type core. Using this structure, the cell conversion efficiency can reach about 7.19%.

Sure, the CNMW structure can be easily prepared by a template method as being done by Jung et al. [83], as illustrated in Fig. 10, where they used the photoresist mask to protect the position on the silicon surface corresponding to the MWs. The representative SEM images of their obtained wafer-scaled CNMW structure are given in Fig. 15b and c.

Recently, Bai et al. [89] developed a simple template-free approach for the fabrication of such CNMW structure by one-step etching. In their process, the etchant is composed of KMnO₄/AgNO₃/HF. The overall formation mechanism of the CNMW structure is illustrated in Fig. 16a. Firstly, many Ag nanoparticles are deposited on the silicon surface via the electroless deposition mechanism; then, the etching reactions started, when the silicon atoms are oxide to SiF₄, which can be easily hydrolyzed to SiF₆²⁻. As the reactions proceed, the concentration of SiF₆²⁻ increases until they nucleate at the silicon surface and grow into H₂SiF₆ particles. These particles can shelter parts of the silver nanoparticles, block the etchant from the contact with the catalysts, thus act as the mask. The obtained CNMW structure is given in Fig. 16b and c.

4.7. Ultra-thin silicon wafer by homogeneous etching

The anisotropic MACE of silicon is the basic reason for the designable fabrication of various novel, controllable silicon

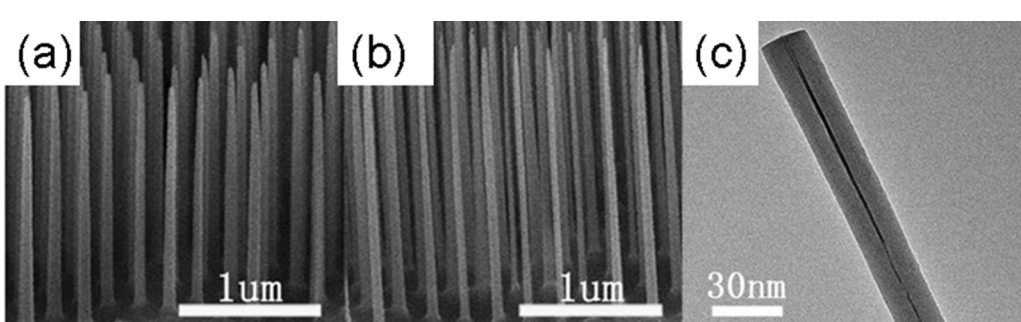


Fig. 14. (a and b) SEM images of SiNW arrays with gradually reduced diameter by a two-step dry oxidation and post-chemical etching process; (c) TEM image of a single core–shell SiNW with inner diameter down to sub-10 nm [66].

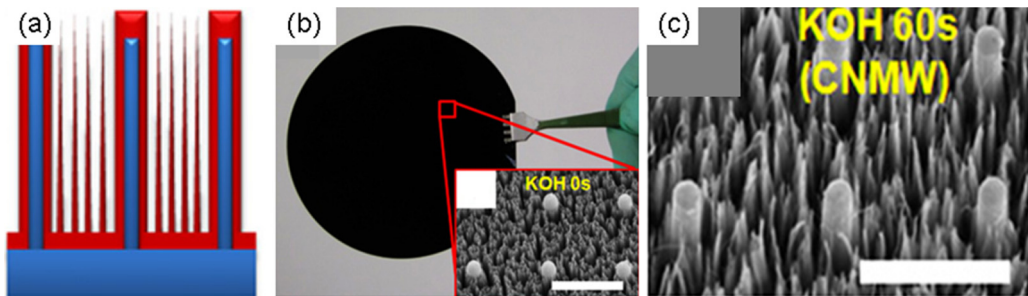


Fig. 15. (a) Illustration of the bulk and radial p–n junctions structure based on CNMW structure (red for the n-type shell and blue for the p-type core), and wafer-scaled CNMW structure (b) before and (c) after KOH process [83]. (For interpretation of the references to color in this figure legend, the reader is referred to the web version of this article.)

nanostructures. On the other hand, this also makes the uniform non-directional etching into difficulty.

Considering the etching directions can be regulated by the etchant concentration, by adjusting the ratio of the HF, AgNO_3 and H_2O_2 in the etchant, Bai et al. [90] realized the homogeneous etching of the silicon wafer. The obtained ultra-thin silicon wafer with thickness about $30 \mu\text{m}$ and average roughness of 13 nm is shown in Fig. 17. This work exploits a new field of application for the MACE method. If such MACE technology is combined with the oxidation and post-chemical etching process mentioned above, it will be very possible to realize the fabrication of ultra-thin silicon wafers with nanoscale thickness.

5. Improved MACE technologies

On the basis of traditional MACE etching technology, some scholars have also conducted further improvements. These efforts contain introducing extra electric field, optical filed, even changing the phase state of the etchant.

5.1. Electric field assisted etching

MACE is a typical electroless galvanic reaction; therefore, it can be also regulated by extra electric field [91,92]. By introducing periodic pulsing of anodic bias during gold-assisted chemical etching of silicon, as shown in Fig. 18a and b, Kim et al. [92] obtained bamboo-like SiNW arrays (Fig. 18c), where the length of every segment is controllable. At the joint positions, the SiNW is porosity-patterned thus can be broken by ultrasonic treatment, which allows as harvesting SiNWs with desired lengths (Fig. 18d).

In this electric field assisted etching process, the extra anodic potential pulses results in sharp increase of current densities during the etching process. These pulsing currents can inject abundant holes into the silicon, which preferentially diffuse to the metal/silicon interface rather than to the solution/silicon interface. This is because the valence band of silicon at the former interface is energetically higher than that at the latter. Such abundant holes accelerate the reaction between the silicon and the HF thus generated porous structures. Therefore, in this novel electric filed

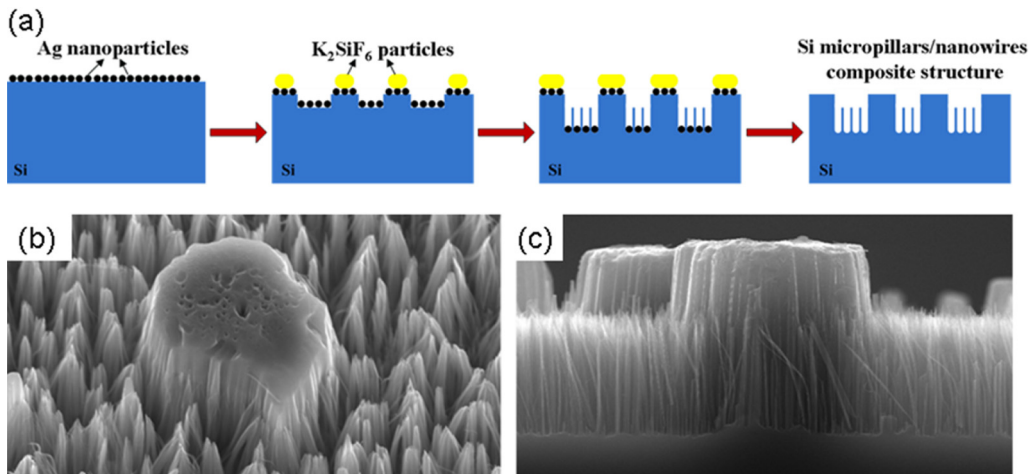


Fig. 16. (a) Formation mechanism of the CNMW structure in the one-step template-free etching method, and (b and c) the SEM images of the obtained CNMW structure [89].

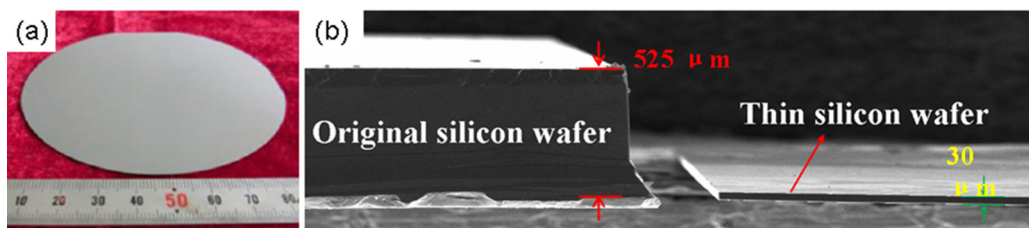


Fig. 17. (a) A picture of 4 in. ultra-thin silicon wafer, and (b) comparison for the thickness of the original and the ultra-thin silicon wafers [90].

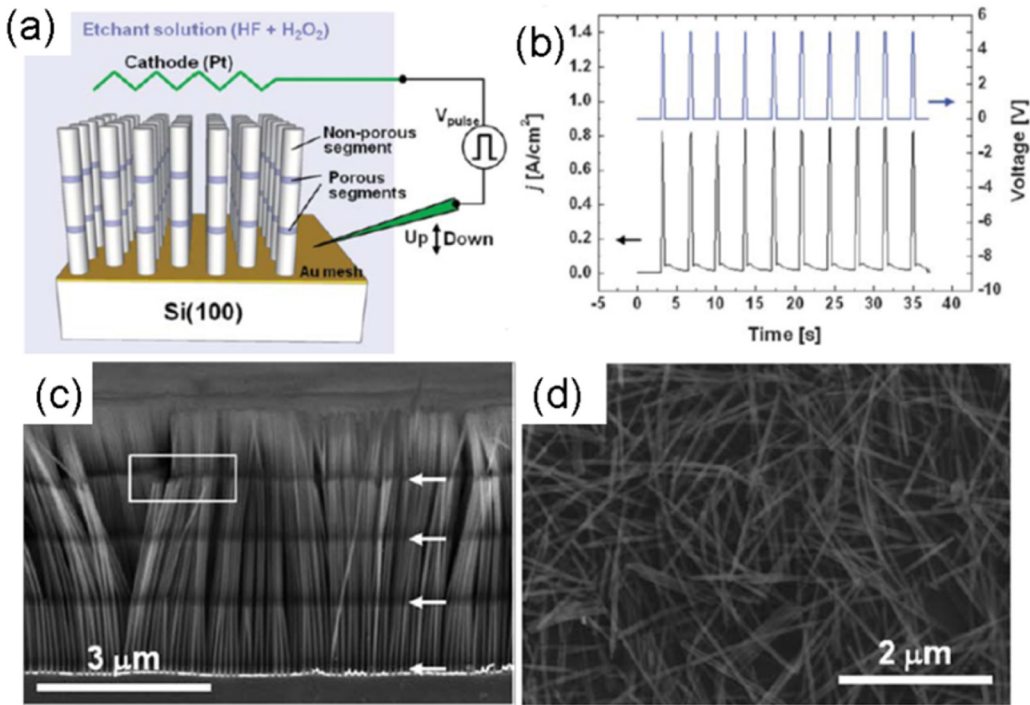


Fig. 18. (a) Illustration of the electrochemical set up employed for introducing periodic pulsing of anodic bias during MACE of silicon, and (b) a typical current-time transient during the etching process; (c) SEM image of SiNW array fabricated by this method, and (d) the SiNWs separated from the samples given in panel c [92].

assisted etching, pulse duration and pulse interval determine the lengths of porous wire segments and nonporous ones, respectively.

5.2. Optical assisted etching

In MACE process, the etching rate dramatically relate to the carrier concentrations at the reaction front. While, due to the intrinsic semiconductor properties of silicon, the carrier concentration can be dramatically enhanced by an irradiation [76]. So introducing extra optical field can also result in great influences on the etching process.

Ding et al. [93] have amplified the influences of the light on silicon etching utilizing the local surface plasmons of Ag nanoparticles. Based on the conventional etching process, they added vertical laser illumination with a wavelength of 476 nm on the silicon surface. As shown in Fig. 19a, the light with this wavelength can excite the local surface plasmons of Ag nanoparticles, which results in strong optical field around the nanoparticle. This enhanced optical field then brings about abundant carriers generated in the silicon substrate around the silver nanoparticles. Such generated carriers, especially holes, can greatly accelerate the etching. The result is that, under the laser illustration, the etching

area and etching rate are both enlarged, and special crateriform morphology is obtained (Fig. 19b); while in the area with no illumination, normal vertical SiNHs are formed (Fig. 19c).

In addition, Lin et al. [94] have also used a light-induced TiO₂ etching technology to fabricate ultra-small surface textures on the silicon surface. Since this method can avoid the introduction of metal impurity, it is of application prospect in fabricating solar cells.

5.3. Vapor phase MACE

Except introducing extra physical fields, Hildreth and Schmidt [18] have also reported a vapor phase MACE (VP-MACE) of Silicon. The schematic of the VP-MACE process is very similar as the conventional MACE one, as given in Fig. 20a. This technology can effectively avoid the influence of the H₂ bubbles on the surface quality of the obtained silicon nanostructures; and circumvent the impact of the fluid flow on the motivation of the catalyst.

The feature resolution of the obtained structure is comparable to the liquid phase MACE and on the order of 1–2 nm (Fig. 20b). By changing the catalyst species, etchant concentration, substrate temperature, they have demonstrated that, this method can also be

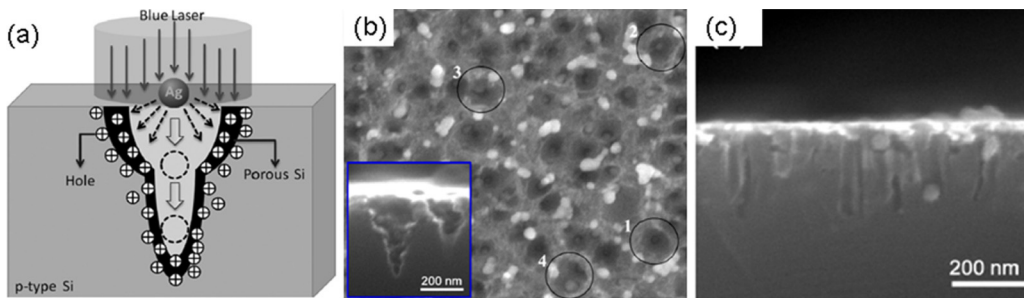


Fig. 19. (a) Schematics of the etching mechanism with laser illumination, and (b) the obtained special crateriform morphology on the silicon surface; (c) normal vertical SiNHs etched in the area with no illumination [93].

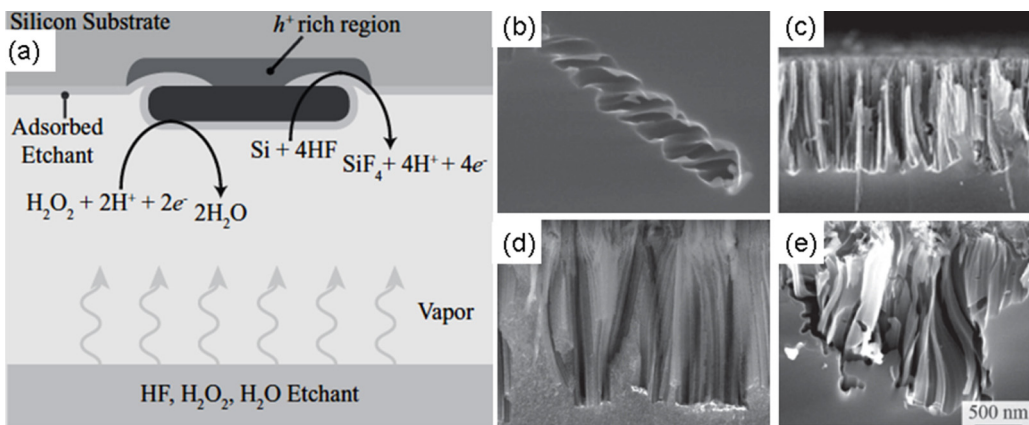


Fig. 20. (a) Schematic of the VP-MACE process; (b) SEM micrograph of silicon nanostructure, which shows high feature resolution, formed after VP-MACE; the fabricated (c) SiNW, (d) vertical SiNHs and (e) helical SiNHs by the VP-MACE process [18].

used to fabricate various silicon nanostructures, like SiNW, vertical and helical SiNHs (Fig. 20c–e).

6. Conclusions

Recent developments in fabricating designable silicon nanostructure using MACE method have been summed up in this article. Based on deeper and deeper understanding on the etching mechanisms during the MACE process, it has been demonstrated that the fundamental for the fabrication of desired silicon nanostructures is the anisotropic etching. That is to say, the Si (100) surface has the fewest silicon back bonds thus should be preferentially etched; while the Si non-(100) surfaces are deprioritized. By regulating the substrate quality, catalyst and etchant, adding post processing, or introducing extra physical fields, such etch anisotropy can be effectively controlled, as the abundant efforts have been made in this field.

Some typically designable silicon nanostructures fabricated using the MACE method, and the recently developed improved MACE processes by introducing extra electric field, optical field, even changing the phase state of the etchant are mainly summarized. From the published reports it was found that, SiNWs (NHs) of specific morphologies, length (depth), density and surface quality have already been fabricated; and the anisotropic etching feature can be overcome thus a homogeneous up to down etching of a silicon wafer has been realized. In addition, the introduction of extra fields and the VP-MACE bring about new vitalities for MACE, which indicate more widespread application of MACE in fabricating specific novel silicon nanostructures.

Acknowledgements

This work is supported partially by National High-tech R&D Program of China (863 Program, No. 2015AA034601), National Natural Science Foundation of China (Grant nos. 91333122, 51402106, 51372082, 51172069, 61204064 and 51202067), Ph.D. Programs Foundation of Ministry of Education of China (Grant nos. 20120036120006, 20130036110012), Par-Eu Scholars Program, and the Fundamental Research Funds for the Central Universities.

References

- [1] I. Zardo, S. Conesa-Boj, S. Estradé, L. Yu, F. Peiro, P.R. Cabarrocas, J. Morante, J.i. Arbiol, A.F. Morral, Growth study of indium-catalyzed silicon nanowires by plasma enhanced chemical vapor deposition, *Appl. Phys. A* 100 (2010) 287–296.
- [2] S. Hofmann, C. Ducati, R. Neill, S. Piscane, A. Ferrari, J. Geng, R. Dunin-Borkowski, J. Robertson, Gold catalyzed growth of silicon nanowires by plasma enhanced chemical vapor deposition, *J. Appl. Phys.* 94 (2003) 6005–6012.
- [3] D. Ma, C. Lee, F. Au, S. Tong, S. Lee, Small-diameter silicon nanowire surfaces, *Science* 299 (2003) 1874–1877.
- [4] J.R. Maiolo, B.M. Kayes, M.A. Filler, M.C. Putnam, M.D. Kelzenberg, H.A. Atwater, N.S. Lewis, High aspect ratio silicon wire array photoelectrochemical cells, *J. Am. Chem. Soc.* 129 (2007) 12346–12347.
- [5] Y. Wu, P. Yang, Direct observation of vapor-liquid-solid nanowire growth, *J. Am. Chem. Soc.* 123 (2001) 3165–3166.
- [6] D. Kwak, H. Cho, W.-C. Yang, Dimensional evolution of silicon nanowires synthesized by Au-Si island-catalyzed chemical vapor deposition, *Physica E* 37 (2007) 153–157.
- [7] J. Bhardwaj, H. Ashraf, A. McQuarrie, Dry silicon etching for MEMS, *Proc. Symp. Microstructures and Microfabricated Systems, ECS*, 1997, pp. 1–13.
- [8] R.M. Ng, T. Wang, F. Liu, X. Zuo, J. He, M. Chan, Vertically stacked silicon nanowire transistors fabricated by inductive plasma etching and stress-limited oxidation, *Electron. Device Lett., IEEE* 30 (2009) 520–522.
- [9] K.-Q. Peng, Y.-J. Yan, S.-P. Gao, J. Zhu, Synthesis of large-area silicon nanowire arrays via self-assembling nanoelectrochemistry, *Adv. Mater.* 14 (2002) 1164.
- [10] K. Peng, J. Hu, Y. Yan, Y. Wu, H. Fang, Y. Xu, S. Lee, J. Zhu, Fabrication of single-crystalline silicon nanowires by scratching a silicon surface with catalytic metal particles, *Adv. Funct. Mater.* 16 (2006) 387–394.
- [11] H. Han, Z. Huang, W. Lee, Metal-assisted chemical etching of silicon and nanotechnology applications, *Nano Today* 9 (2014) 271–304.
- [12] Z. Huang, N. Geyer, L. Liu, M. Li, P. Zhong, Metal-assisted electrochemical etching of silicon, *Nanotechnology* 21 (2010) 465301.
- [13] W. Chern, K. Hsu, I.S. Chun, B.P.d. Azeredo, N. Ahmed, K.-H. Kim, J.-m. Zuo, N. Fang, P. Ferreira, X. Li, Nonlithographic patterning and metal-assisted chemical etching for manufacturing of tunable light-emitting silicon nanowire arrays, *Nano Lett.* 10 (2010) 1582–1588.
- [14] J. Tang, J. Shi, L. Zhou, Z. Ma, Fabrication and optical properties of silicon nanowires arrays by electroless Ag-catalyzed etching, *Nano-Micro Lett.* 3 (2011) 129–134.
- [15] J. Huang, S.Y. Chiam, H.H. Tan, S. Wang, W.K. Chim, Fabrication of silicon nanowires with precise diameter control using metal nanodot arrays as a hard mask blocking material in chemical etching, *Chem. Mater.* 22 (2010) 4111–4116.
- [16] X. Geng, M. Li, L. Zhao, P.W. Bohn, Metal-assisted chemical etching using Tollens's reagent to deposit silver nanoparticle catalysts for fabrication of quasi-ordered silicon micro/nanostructures, *J. Electron. Mater.* 40 (2011) 2480–2485.
- [17] K. Peng, Z. Huang, J. Zhu, Fabrication of large-area silicon nanowire p-n junction diode arrays, *Adv. Mater.* 16 (2004) 73–76.
- [18] O.J. Hildreth, D.R. Schmidt, Vapor phase metal-assisted chemical etching of silicon, *Adv. Funct. Mater.* 24 (2014) 3827–3833.
- [19] Z. Huang, N. Geyer, P. Werner, J.U. De Boor Gösele, Metal-assisted chemical etching of silicon: a review, *Adv. Mater.* 23 (2011) 285–308.
- [20] C.Q. Lai, H. Cheng, W. Choi, C.V. Thompson, Mechanics of catalyst motion during metal assisted chemical etching of silicon, *J. Phys. Chem. C* 117 (2013) 20802–20809.
- [21] O.J. Hildreth, W. Lin, C.P. Wong, Effect of catalyst shape and etchant composition on etching direction in metal-assisted chemical etching of silicon to fabricate 3D nanostructures, *ACS Nano* 3 (2009) 4033–4042.
- [22] N. Geyer, N. Wollschläger, B. Fuhrmann, A. Tonkikh, A. Berger, P. Werner, M. Jungmann, R. Krause-Rehberg, H.S. Leipner, Influence of the doping level on the porosity of silicon nanowires prepared by metal-assisted chemical etching, *Nanotechnology* 26 (2015) 245301.
- [23] C. Canevali, M. Alia, M. Fanciulli, M. Longo, R. Ruffo, C. Mari, Influence of doping elements on the formation rate of silicon nanowires by silver-assisted chemical etching, *Surf. Coat. Technol.* 280 (2015) 37–42.
- [24] H. Asoh, F. Arai, S. Ono, Effect of noble metal catalyst species on the morphology of macroporous silicon formed by metal-assisted chemical etching, *Electrochim. Acta* 54 (2009) 5142–5148.

- [25] Z. Huang, T. Shimizu, S. Senz, Z. Zhang, N. Geyer, U. Gösele, Oxidation rate effect on the direction of metal-assisted chemical and electrochemical etching of silicon, *J. Phys. Chem. C* 114 (2010) 10683–10690.
- [26] P. Lianto, S. Yu, J. Wu, C. Thompson, W. Choi, Vertical etching with isolated catalysts in metal-assisted chemical etching of silicon, *Nanoscale* 4 (2012) 7532–7539.
- [27] F. Bai, M. Li, D. Song, H. Yu, B. Jiang, Y. Li, One-step synthesis of lightly doped porous silicon nanowires in HF/AgNO₃/H₂O₂ solution at room temperature, *J. Solid State Chem.* 196 (2012) 596–600.
- [28] S.-C. Shiu, S.-B. Lin, S.-C. Hung, C.-F. Lin, Influence of pre-surface treatment on the morphology of silicon nanowires fabricated by metal-assisted etching, *Appl. Surf. Sci.* 257 (2011) 1829–1834.
- [29] F. Bai, M. Li, R. Huang, Y. Yu, T. Gu, Z. Chen, H. Fan, B. Jiang, Wafer-scale fabrication of uniform Si nanowire arrays using the Si wafer with UV/ozone pretreatment, *J. Nanopart. Res.* 15 (2013) 1–7.
- [30] D. Wang, R. Ji, S. Du, A. Albrecht, P. Schaa, Ordered arrays of nanoporous silicon nanopillars and silicon nanopillars with nanoporous shells, *Nanoscale Res. Lett.* 8 (2013) 1–9.
- [31] C. Chartier, S. Bastide, C. Lévy-Clément, Metal-assisted chemical etching of silicon in HF-H₂O₂, *Electrochim. Acta* 53 (2008) 5509–5516.
- [32] K. Balasundaram, J.S. Sadhu, J.C. Shin, B. Azeredo, D. Chanda, M. Malik, K. Hsu, J. A. Rogers, P. Ferreira, S. Sinha, Porosity control in metal-assisted chemical etching of degenerately doped silicon nanowires, *Nanotechnology* 23 (2012) 305304.
- [33] K. Peng, Y. Wu, H. Fang, X. Zhong, Y. Xu, J. Zhu, J. Uniform, Axial-orientation alignment of one-dimensional single-crystal silicon nanostructure arrays, *Angew. Chem. Int. Ed.* 44 (2005) 2737–2742.
- [34] P. Werner, C.C. Büttner, L. Schubert, G. Gerth, N.D. Zakarov, U. Gösele, Gold-enhanced oxidation of silicon nanowires, *Int. J. Mater. Res.* 98 (2007) 1066–1070.
- [35] Y. Li, M. Li, R. Li, P. Fu, L. Chu, D. Song, Method to determine the optimal silicon nanowire length for photovoltaic devices, *Appl. Phys. Lett.* 106 (2015) 091908.
- [36] Y. Li, M. Li, R. Li, P. Fu, B. Jiang, D. Song, C. Shen, Y. Zhao, R. Huang, Linear length-dependent light-harvesting ability of silicon nanowire, *Opt. Commun.* 355 (2015) 6–9.
- [37] Z. Duan, M. Li, T. Mwenya, F. Bai, Y. Li, D. Song, Geometric parameter optimization to minimize the light-reflection losses of regular vertical silicon nanorod arrays used for solar cells, *Phys. Status Solidi* 211 (2014) 2527–2531.
- [38] Z. Duan, M. Li, T. Mwenya, P. Fu, Y. Li, D. Song, Effective light absorption and its enhancement factor for silicon nanowire-based solar cell, *Appl. Opt.* 55 (2016) 117–121.
- [39] L. Cao, J.S. White, J.-S. Park, J.A. Schuller, B.M. Clemens, M.L. Brongersma, Engineering light absorption in semiconductor nanowire devices, *Nat. Mater.* 8 (2009) 643–647.
- [40] E. Garnett, P. Yang, Light trapping in silicon nanowire solar cells, *Nano Lett.* 10 (2010) 1082–1087.
- [41] H. Bao, W. Zhang, L. Chen, H. Huang, C. Yang, X. Ruan, An investigation of the optical properties of disordered silicon nanowire mats, *J. Appl. Phys.* 112 (2012) 124301.
- [42] S.-K. Kim, R.W. Day, J.F. Cahoon, T.J. Kempa, K.-D. Song, H.-G. Park, C.M. Lieber, Tuning light absorption in core/shell silicon nanowire photovoltaic devices through morphological design, *Nano Lett.* 12 (2012) 4971–4976.
- [43] T. Song, S.-T. Lee, B. Sun, Silicon nanowires for photovoltaic applications: The progress and challenge, *Nano Energy* 1 (2012) 654–673.
- [44] J.K. Mann, R. Kurstjens, G. Pourtois, M. Gilbert, F. Dross, J. Poortmans, Opportunities in nanometer sized Si wires for PV applications, *Progress Mater. Sci.* 58 (2013) 1361–1387.
- [45] X. Wang, K.-Q. Peng, Y. Hu, F.-Q. Zhang, B. Hu, L. Li, M. Wang, X.-M. Meng, S.-T. Lee, Silicon/Hematite core/shell nanowire array decorated with gold nanoparticles for unbiased solar water oxidation, *Nano Lett.* 14 (2013) 18–23.
- [46] G.-L. Zang, G.-P. Cheng, C. Shi, Y.-K. Wang, W.-W. Li, H.-Q. Yu, A bio-photoelectrochemical cell with a MoS₃-modified silicon nanowire photocathode for hydrogen and electricity production, *Energy Environ. Sci.* 7 (2014) 3033–3039.
- [47] Y. Li, M. Li, D. Song, H. Liu, B. Jiang, F. Bai, L. Chu, Broadband light-concentration with near-surface distribution by silver capped silicon nanowire for high-performance solar cells, *Nano Energy* 11 (2015) 756–764.
- [48] T.-C. Yang, T.-Y. Huang, H.-C. Lee, T.-J. Lin, T.-J. Yen, Applying silicon nanoholes with excellent antireflection for enhancing photovoltaic performance, *J. Electrochem. Soc.* 159 (2011) B104–B108.
- [49] J. Oh, H.-C. Yuan, H.M. Branz, An 18.2%-efficient black-silicon solar cell achieved through control of carrier recombination in nanostructures, *Nat. Nanotechnol.* 7 (2012) 743–748.
- [50] H.-C. Yuan, V.E. Yost, M.R. Page, P. Stradins, D.L. Meier, H.M. Branz, Efficient black silicon solar cell with a density-graded nanoporous surface: optical properties, performance limitations, and design rules, *Appl. Phys. Lett.* 95 (2009) 123501.
- [51] T.-Y. Huang, T.-J. Yen, MRS Proceedings. mrsf10-1302-w1309-1304, Cambridge Univ. Press.
- [52] C.Y. Chen, C.S. Wu, C.J. Chou, T.J. Yen, Morphological control of single-crystalline silicon nanowire arrays near room temperature, *Adv. Mater.* 20 (2008) 3811–3815.
- [53] L. Li, Y. Liu, X. Zhao, Z. Lin, C.-P. Wong, Uniform vertical trench etching on silicon with high aspect ratio by metal-assisted chemical etching using nanoporous catalysts, *ACS Appl. Mater. Interfaces* 6 (2013) 575–584.
- [54] K. Peng, M. Zhang, A. Lu, N.-B. Wong, R. Zhang, S.-T. Lee, Ordered silicon nanowire arrays via nanosphere lithography and metal-induced etching, *Appl. Phys. Lett.* 90 (2007) 163123.
- [55] X. Geng, Z. Qi, M. Li, B.K. Duan, L. Zhao, P.W. Bohn, Fabrication of antireflective layers on silicon using metal-assisted chemical etching with in situ deposition of silver nanoparticle catalysts, *Sol. Energy Mater. Sol. C* 103 (2012) 98–107.
- [56] B. Jiang, M. Li, F. Bai, H. Yu, T. Mwenya, Y. Li, D. Song, Morphology-controlled synthesis of silver nanoparticles on the silicon substrate by a facile silver mirror reaction, *ALP Adv.* 3 (2013) 032119.
- [57] B. Jiang, M. Li, D. Song, Y. Li, T. Mwenya, Facile deposition of ultrafine silver particles on silicon surface not submerged in precursor solutions for applications in antireflective layer, *J. Nanomater.* 2014 (2014).
- [58] B. Jiang, M. Li, Y. Li, D. Song, T. Mwenya, Vertical deposition of ultrafine silver particles on silicon surface out of solutions by silver mirror process, *Mater. Lett.* 116 (2014) 195–198.
- [59] B. Jiang, M. Li, D. Song, Y. Li, T. Mwenya, A facile direct deposition of silver nanoparticles on silicon surface by silver mirror process, *Crystal Res. Technol.* 48 (2013) 1044–1049.
- [60] Z. Huang, T. Shimizu, S. Senz, Z. Zhang, X. Zhang, W. Lee, N. Geyer, U. Gösele, Ordered arrays of vertically aligned [110] silicon nanowires by suppressing the crystallographically preferred <100> etching directions, *Nano Lett.* 9 (2009) 2519–2525.
- [61] Bing Jiang, Meicheng Li, Yu Liang, Yang Bai, Dandan Song, Yingfeng Li, J. Lou, Etching anisotropy mechanisms lead to the morphology-controlled silicon nanoporous structures by metal assisted chemical etching, *Nanoscale* (2015), doi:<http://dx.doi.org/10.1039/C5NR07327H>.
- [62] X.H. Liu, H. Zheng, L. Zhong, S. Huang, K. Karki, L.Q. Zhang, Y. Liu, A. Kushima, W. T. Liang, J.W. Wang, Anisotropic swelling and fracture of silicon nanowires during lithiation, *Nano Lett.* 11 (2011) 3312–3318.
- [63] S. Cheng, C. Chung, H. Lee, A study of the synthesis, characterization, and kinetics of vertical silicon nanowire arrays on (001) Si substrates, *J. Electrochem. Soc.* 155 (2008) D711–D714.
- [64] I. Lombardi, A.I. Hochbaum, P. Yang, C. Carraro, R. Maboudian, Synthesis of high density, size-controlled Si nanowire arrays via porous anodic alumina mask, *Chem. Mater.* 18 (2006) 988–991.
- [65] K.J. Morton, G. Nieberg, S. Bai, S.Y. Chou, Wafer-scale patterning of sub-40 nm diameter and high aspect ratio (>50:1) silicon pillar arrays by nanoimprint and etching, *Nanotechnology* 19 (2008) 345301.
- [66] S. Su, L. Lin, Z. Li, J. Feng, Z. Zhang, The fabrication of large-scale sub-10-nm core-shell silicon nanowire arrays, *Nanoscale Res. Lett.* 8 (2013) 1–7.
- [67] B. Cai, B. Jia, J. Fang, G. Hou, X. Zhang, Y. Zhao, M. Gu, Entire band absorption enhancement in double-side textured ultrathin solar cells by nanoparticle imprinting, *J. Appl. Phys.* 117 (2015) 223102.
- [68] J.-Y. Chen, C. Con, M.-H. Yu, B. Cui, K.W. Sun, Efficiency enhancement of PEDOT:PSS/Si hybrid solar cells by using nanostructured radial junction and antireflective surface, *ACS Appl. Mater. Interfaces* 5 (2013) 7552–7558.
- [69] Y. Li, B. Qian, C. Li, J. Xu, C. Jiang, Optical properties of nanocrystal-silicon thin films on silicon nanopillar arrays after thermal annealing, *Appl. Surf. Sci.* 265 (2013) 324–328.
- [70] A.R. Madaria, M. Yao, C. Chi, N. Huang, C. Lin, R. Li, M.L. Povinelli, P.D. Dapkus, C. Zhou, Toward optimized light utilization in nanowire arrays using scalable nanosphere lithography and selected area growth, *Nano Lett.* 12 (2012) 2839–2845.
- [71] J. Yeom, D. Ratchford, C.R. Field, T.H. Brintlinger, P.E. Pehrsson, Decoupling diameter and pitch in silicon nanowire arrays made by metal-assisted chemical etching, *Adv. Funct. Mater.* 24 (2014) 106–116.
- [72] Z. Huang, H. Fang, J. Zhu, Fabrication of silicon nanowire arrays with controlled diameter, length, and density, *Adv. Mater.* 19 (2007) 744–748.
- [73] P. Gao, J. He, S. Zhou, X. Yang, S. Li, J. Sheng, D. Wang, T. Yu, J. Ye, Y. Cui, Large-area nanosphere self-assembly by a micro-propulsive injection method for high throughput periodic surface nanotexturing, *Nano Lett.* 15 (2015) 4591–4598.
- [74] R. Liu, F. Zhang, C. Con, B. Cui, B. Sun, Lithography-free fabrication of silicon nanowire and nanohole arrays by metal-assisted chemical etching, *Nanoscale Res. Lett.* 8 (2013) 1–8.
- [75] Y. Cho, M. Gwon, H.-H. Park, J. Kim, D.-W. Kim, Wafer-scale nanoconical frustum array crystalline silicon solar cells: promising candidates for ultrathin device applications, *Nanoscale* 6 (2014) 9568–9573.
- [76] Y. Li, M. Li, P. Fu, R. Li, D. Song, C. Shen, Y. Zhao, A comparison of light-harvesting performance of silicon nanocones and nanowires for radial-junction solar cells, *Sci. Rep.* (2015) 5.
- [77] Y. Lu, A. Lal, High-efficiency ordered silicon nano-conical-frustum array solar cells by self-powered parallel electron lithography, *Nano Lett.* 10 (2010) 4651–4656.
- [78] H. Lin, H.-Y. Cheung, F. Xiu, F. Wang, S. Yip, N. Han, T. Hung, J. Zhou, J.C. Ho, C.-Y. Wong, Developing controllable anisotropic wet etching to achieve silicon nanorods, nanopencils and nanocones for efficient photon trapping, *J. Mater. Chem. A* 1 (2013) 9942–9946.
- [79] F. Bai, M. Li, R. Huang, Y. Li, M. Trevor, K.P. Musselman, A one-step template-free approach to achieve tapered silicon nanowire arrays with controllable filling ratios for solar cell applications, *RSC Adv.* 4 (2014) 1794–1798.

- [80] C.-L. Lee, K. Tsujino, Y. Kanda, S. Ikeda, M. Matsumura, Pore formation in silicon by wet etching using micrometre-sized metal particles as catalysts, *J. Mater. Chem.* 18 (2008) 1015–1020.
- [81] J.-Y. Jung, Z. Guo, S.-W. Jee, H.-D. Um, K.-T. Park, J.-H. Lee, A strong antireflective solar cell prepared by tapering silicon nanowires, *Opt. Express* 18 (2010) A286–A292.
- [82] Y. Hung Jr, S.-L. Lee, K.-C. Wu, Y. Tai, Y.-T. Pan, Antireflective silicon surface with vertical-aligned silicon nanowires realized by simple wet chemical etching processes, *Opt. Express* 19 (2011) 15792–15802.
- [83] J.-Y. Jung, Z. Guo, S.-W. Jee, H.-D. Um, K.-T. Park, M.S. Hyun, J.M. Yang, J.-H. Lee, A waferscale Si wire solar cell using radial and bulk p–n junctions, *Nanotechnology* 21 (2010) 445303.
- [84] J. Kim, Y.H. Kim, S.-H. Choi, W. Lee, Curved silicon nanowires with ribbon-like cross sections by metal-assisted chemical etching, *ACS Nano* 5 (2011) 5242–5248.
- [85] S. You, M. Choi, Numerical simulation of microscopic motion and deposition of nanoparticles via electrodynamic focusing, *J. Aerosol Sci.* 38 (2007) 1140–1149.
- [86] J. Sullivan, R. Tung, M. Pinto, W. Graham, Electron transport of inhomogeneous Schottky barriers: a numerical study, *J. Appl. Phys.* 70 (1991) 7403–7424.
- [87] J.M. Weisse, D.R. Kim, C.H. Lee, X. Zheng, Vertical transfer of uniform silicon nanowire arrays via crack formation, *Nano Lett.* 11 (2011) 1300–1305.
- [88] Ruike Li, M. Li, Y. Li, P. Fu, Y. Luo, H. Rui, D. Song, J.M. Mbenque, Co-catalytic mechanism of Au and Ag in silicon etching to fabricate novel nanostructures, *RSC Adv.* 5 (2015) 96483–96487.
- [89] F. Bai, M. Li, R. Huang, D. Song, B. Jiang, Y. Li, Template-free fabrication of silicon micropillar/nanowire composite structure by one-step etching, *Nanoscale Res. Lett.* 7 (2012) 1–5.
- [90] F. Bai, M. Li, D. Song, H. Yu, B. Jiang, Y. Li, Metal-assisted homogeneous etching of single crystal silicon: a novel approach to obtain an ultra-thin silicon wafer, *Appl. Surf. Sci.* 273 (2013) 107–110.
- [91] P.-H. Tseng, W.-C. Tian, S.C. Pan, J.-G. Hwu, Formation of single crystal Si-nanowire by electric field self-redistribution effect in anodic oxidation for multilayer array application, *Nanotechnol. IEEE Trans.* 13 (2014) 1084–1087.
- [92] J. Kim, H. Rhu, W. Lee, A continuous process for Si nanowires with prescribed lengths, *J. Mater. Chem.* 21 (2011) 15889–15894.
- [93] R. Ding, H. Dai, M. Li, J. Huang, Y. Li, M. Trevor, K.P. Musselman, The application of localized surface plasmons resonance in Ag nanoparticles assisted Si chemical etching, *Appl. Phys. Lett.* 104 (2014) 011602.
- [94] Y. Lin, Y. Gao, R. Jia, H. Li, B. Dou, Z. Jin, X. Liu, T. Ye, Solar Cells with ultra-small surface textures fabricated by light-induced TiO₂ etching, *J. Chin. Ceram. Soc.* 40 (2012) 1036–1039.